

D. Ultra-High Resolution Electron Microscopy for Characterization of Catalyst Microstructures and Deactivation Mechanisms

*L. F. Allard, D. A. Blom, D. W. Coffey, C. K. Narula, and M. A. O'Keefe**

Oak Ridge National Laboratory

P.O. Box 2008, MS-6064

Oak Ridge, TN 37831-6064

**Materials Sciences Division, Lawrence Berkeley National Laboratory, Berkeley, CA 94720*

DOE Technology Development Area Specialist: James J. Eberhardt

(202) 586-9837; fax: (202) 586-1600; e-mail: james.eberhardt@ee.doe.gov

ORNL Technical Advisor: D. Ray Johnson

(865) 576-6832; fax: (865) 574-6098; e-mail: johnsondr@ornl.gov

Contractor: Oak Ridge National Laboratory, Oak Ridge, Tennessee

Contract No.: DE-AC05-00OR22725

Objectives

- Develop and utilize new capabilities and techniques for ultra-high resolution transmission electron microscopy (UHR-TEM) to characterize the microstructures of catalytic materials of interest for reduction of NO_x emissions in diesel and automotive exhaust systems.
- Relate the effects of reaction conditions on the changes in morphology of heavy metal species on “real” catalyst support materials (typically oxides).
- Develop capability to experimentally study the effects of experimental reaction treatments on TEM samples of NO_x trap catalyst materials before and after reactions, using the High-Temperature Materials Laboratory (HTML) “ex-situ” catalyst reactor with a specimen holder designed for use in the aberration-corrected electron microscope (ACEM).

Approach

- Utilize Oak Ridge National Laboratory ACEM to characterize for the first time the atomic morphology of heavy-metal species such as platinum and rhenium on oxide support materials via techniques of annular dark-field (ADF) or “Z-contrast” imaging.
- Utilize dedicated scanning transmission electron microscope (STEM) instrument and techniques of spectrum imaging to characterize the structure and chemistry of a series of lean NO_x trap (LNT) and diesel particulate NO_x reduction (DPNR) filter samples being studied by Ford Research Laboratory colleagues.

Accomplishments

- Characterized the morphologies of tri-rhenium carbonyl clusters on gamma-alumina support material, at the atomic level to demonstrate for the first time the unambiguous imaging of clusters of known structure.
- Characterized the nature of platinum catalyst structures on mixed-oxide support materials, including the imaging of platinum species dispersed as single atoms and in precrystalline clusters known as “rafts.”
- Performed initial analysis of the structures of several manufacturers’ NO_x trap and DPNR filter materials, in the as-manufactured condition and after an initial “de-greening” process.

- Demonstrated the potential for the Z-contrast atomic imaging process to allow determination of the precise shapes of nanoparticles and clusters.
- Developed and fabricated a new specimen rod and modifications to the HTML ex-situ reactor system to permit catalyst reaction studies using the ACEM.

Future Direction

- Focus on the use of the ACEM to characterize the location of sulfur species on NO_x reduction catalyst materials, to enable characterization of the mechanisms of sulfur poisoning of these materials. This will involve not only imaging of the catalysts at the single-atom level, but also the use of the electron spectroscopy capabilities on the ACEM to obtain chemical information at the atomic level.
- Continue to work on the critical problem of determination of precise shapes of catalyst nanoparticles to determine the most important characteristics for control of catalytic performance.
- Extend new imaging and spectroscopy techniques to include studies of bi-metallic catalyst particles (e.g., gold-palladium).

Technical Progress

Imaging of ultrafine atomic clusters of heavy metals on low atomic number supports is expected to be significantly enhanced with the advent of research on the new aberration-corrected STEM/TEM electron microscope (JEOL 2200FS-AC “ACEM”). In this report, we illustrate the potential for imaging atomic species down to the single atom level, with samples of platinum on thin carbon films, platinum on and rhenium on alumina. The latter samples are part of a specimen suite comprising primarily tri-rhenium carbonyl clusters on gamma alumina, provided by Prof. B. C. Gates and students at UCaldavis. Details of the changes in cluster morphology related to decarbonylation experiments in an ex-situ reactor system will be reported by Narula, Moses, and Allard in a separate quarterly. Platinum on carbon samples were prepared by sputter deposition from a platinum target using argon ions, in our ion-sputtering unit. The ultra-thin carbon films were prepared by controlled evaporation of carbon onto NaCl substrates, then floating films (nominally 10Å to 15Å thick) on water, and picking the thin films up on holey carbon support films. The thin carbon is essentially not imaged in the ADF imaging mode of the ACEM, allowing only platinum atoms and clusters to be revealed in bright contrast.

The platinum on carbon experiment was conducted using two specimens. One sample was prepared using dual-gun sputtering for 20 s under standard beam energy conditions. The second sample was prepared using identical beam

conditions, but only a single gun, giving nominally one-half the amount of platinum species on the carbon film surface. The ACEM was adjusted to achieve a fully corrected electron probe, using an illuminating aperture that calculated to produce a beam diameter of just about 1 Å.

Platinum/carbon imaging results: Figures 1 and 2 show the ADF images of the 1-gun and 2-gun depositions, respectively. Single atoms and “rafts” of atoms having 2–3 layers are seen in both samples. It is clear that there is a direct correlation between the deposition parameters and the relative amounts of platinum observed on the respective samples. Also note that these images were acquired prior to achieving fully stable operation on the instrument, and also while using a nonideal aperture size in the probe-forming lens system, so that no better than 1-Å resolution was expected. The line profile shown over a single platinum atom (raw data) indicates just over 1Å in diameter, as expected. The impressive result from this experiment is that we expect to be able to image single atoms of a heavy element with a resolution significantly lower than the expected 0.7-Å ultimate resolution of the microscope. A second observation (not illustrated here) is that the atoms and clusters are mobile on the surface of the carbon film and continually change position between successive image acquisitions. This phenomenon is not unexpected and has been observed in other sample types observed to date, including the rhenium on alumina samples described below. It is important to be able to (eventually) determine the relationship between images recorded at highest resolution on

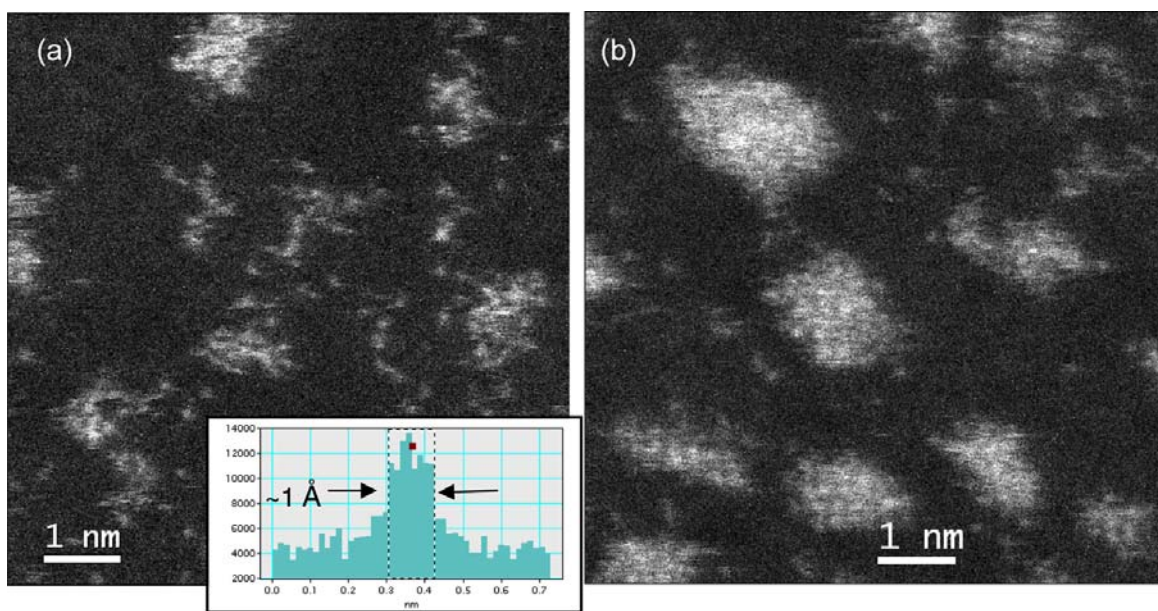


Figure 1. (a) Platinum sputtered onto thin carbon film, showing single atoms, clusters, and “rafts.” (b) A second sputter coating of a carbon film with platinum, accumulating about double the total platinum relative to the first coating. Rafts are larger and fewer clusters are present, but no discrete crystallinity is evident even in the larger rafts.

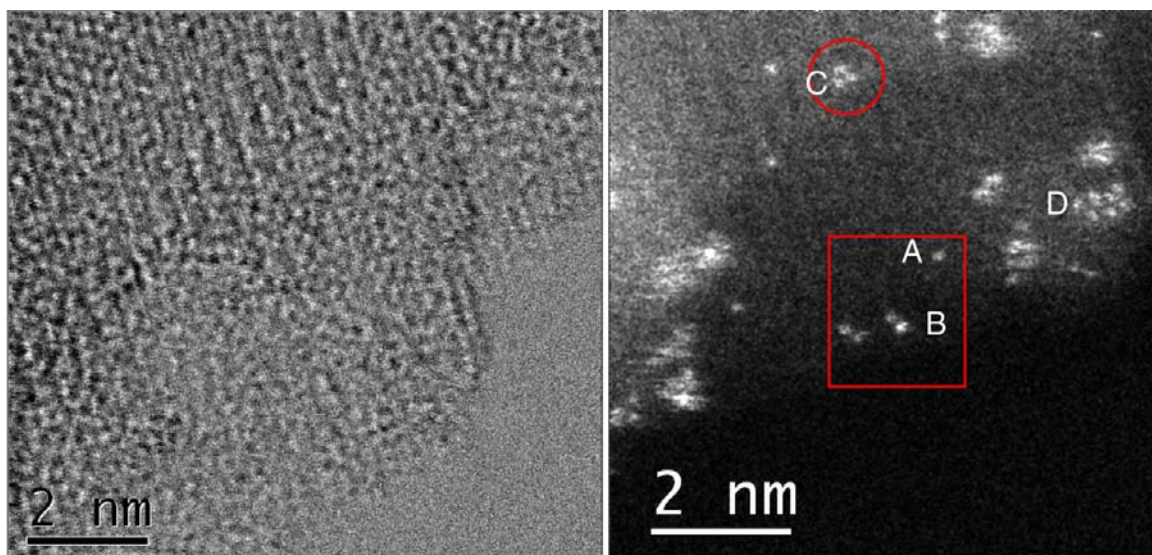


Figure 2. (a) BF image of thin plate of γ - Al_2O_3 , decorated with rhenium atoms. The phase contrast from the alumina obscures unambiguous determination of location of rhenium species. (b) Same area in ADF image, showing rhenium species in bright contrast. Single atom at A, apparent dimmer at B, clear trimer at C, small raft of atoms at D.

the ACEM and the original distribution of atoms and clusters on as-prepared catalyst specimens. Correlation of imaged morphologies with results from other measurement techniques, again as being done in the work with UCAlDavis, may prove the most valuable

for providing a reliable quantification of cluster morphologies and distributions.

Rhenium/ γ - Al_2O_3 imaging results: Figure 2 is a bright-field (BF) STEM image of a thin γ - Al_2O_3 flake, showing high phase contrast and an inability

to unambiguously distinguish the precise location of rhenium atoms and tri-rhenium clusters. The ADF image of the exact same sample area is shown in Figure 3, where the rhenium species are clearly seen in bright contrast. These images were also acquired with a probe diameter of about 1 Å. A single atom (A), an apparent dimer (B) and a tri-rhenium cluster (C) are seen (the raw digital images were smoothed using a 3×3 filter). Interestingly, one atom of the “dimer” is brighter in contrast than the other; an intensity profile (Figure 4) shows double the intensity in the bright atom, which is consistent with the intensity which would result from two atoms, one above the other, in the trimer arrangement shown in the cartoon. It is therefore likely that the dimer is actually a trimer seen precisely on edge, a configuration possible if the trimer were attached to a ledge on the alumina support just a few Ångströms in height. The trimer at C shows equal intensity for the individual atoms and is therefore a classical tri-rhenium cluster. The atom-atom spacing in trimer C is slightly different than the spacings in a nearby

cluster D (2.0 \AA vs 2.3 \AA), suggesting that the rhenium atoms (perhaps still carbonylated) are influenced by the crystallography of the γ -alumina crystal lattice. Direct observations of atoms and clusters such as illustrated here, made possible by the new generation of aberration-corrected electron microscopes, and coupled with molecular simulations, offer the potential for a deeper understanding of the changes in morphology of heavy metal species in catalyst systems with aging treatments.

Characterization of fine particle morphology:

The direct relationship in the ADF image between number of atoms in a column and the intensity of the column was shown clearly in the example of the tri-rhenium cluster on edge above. In our FY 2004 annual report we also demonstrated this effect for an ideal TEM image of a platinum cube-octahedron. Here we show a bright-field (BF) image of a 7-nm gold particle supported on a 10-nm-thick amorphous carbon film, processed to extract the so-called “exit surface wave” image, at a resolution in the 1-Å range. The problem with the BF images is that the

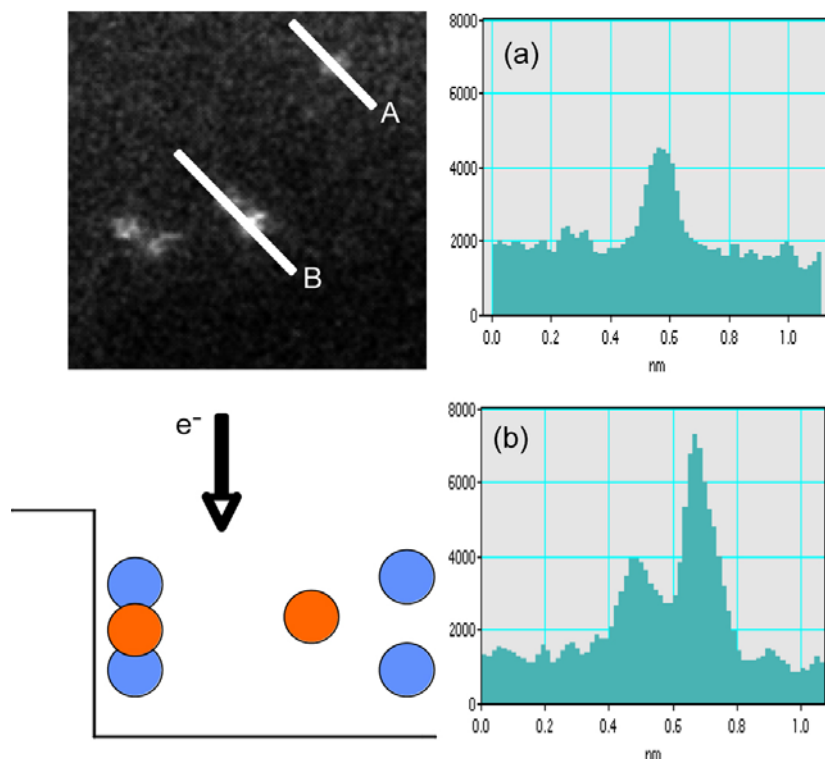


Figure 3. Analysis of the dimer at B shows one “atom” is twice the intensity of the adjacent, where the adjacent atom intensity profile is precisely the height of the single atom at A. This suggests the dimer is actually a trimer tethered to a ledge in the alumina surface and is oriented edge-on to the electron beam, as indicated by the cartoon.

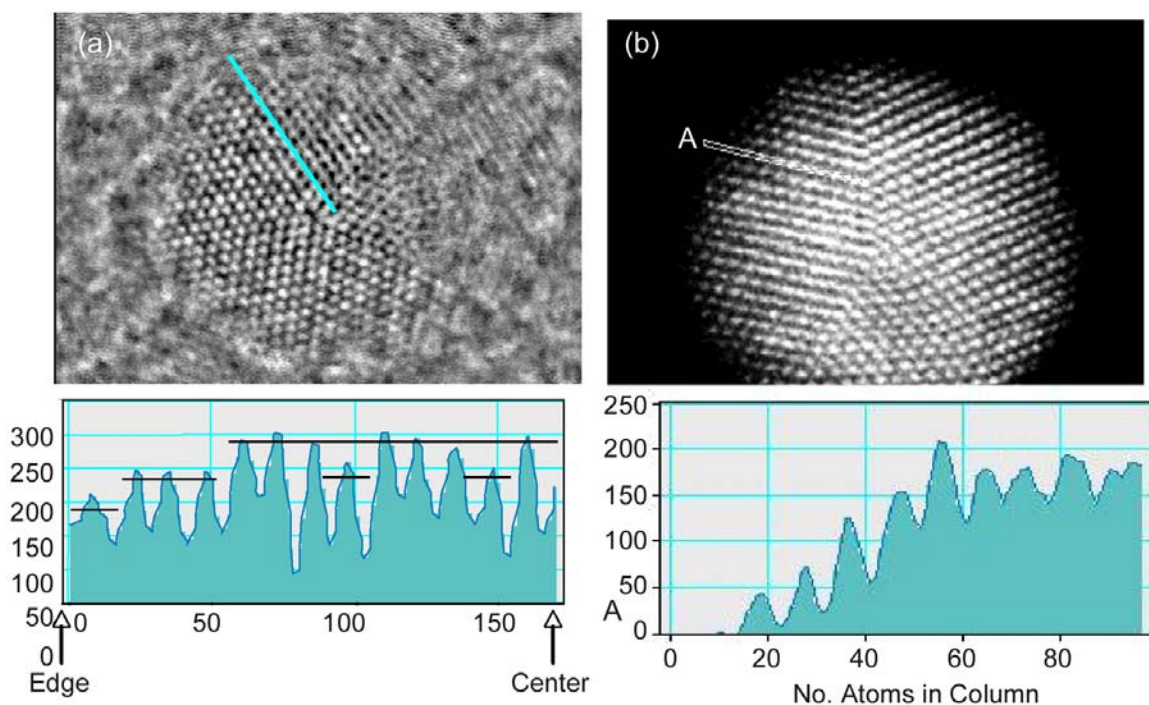


Figure 4. (a) Reconstructed BF Exit Surface Wave image of 7-nm gold particle, with intensity profile inset. The profile shows discrete steps in intensity column by column, but the carbon background makes interpretation ambiguous. (b) Direct ADF image from STEM, with intensity profile A showing number of atoms column by column.

phase contrast from the carbon film makes a significant contribution to the contrast of the atomic columns in the particle. However, in ADF images, because of its very low scattering power relative to the high atomic number of the heavy metal particle, the carbon film contributes essentially no signal to the image. Figure 4 compares the gold particle on carbon in BF [Figure 4(a)] with the gold particle on carbon [Figure 4(b)] in the ADF aberration-corrected STEM image. Because of the phase contrast due to the carbon film in the BF image, the interpretation of discrete intensity jumps column to column are ambiguous. However, a line profile along a typical row of atoms in the gold particle ADF image shows the discrete jumps from column to column. One possible interpretation of the number of atoms in the individual columns is given on the profile inset in Figure 4(b). These are the most promising results obtained to date that show the possibility for ADF imaging in the ACEM to allow full determination of the precise shape of nanometer-sized catalyst particles. Further work is needed to work out image processing methods to allow automatic analysis of particle shapes from ADF images.

Development of new reactor specimen rod: To conduct catalyst reaction experiments involving examination of catalyst powder samples in the ACEM before and after reaction in the HTML ex-situ catalyst reactor system, a new specimen rod for the ACEM had to be designed and fabricated. The new rod was built with the capability to protect the catalyst specimen from atmospheric exposure during transfer of the sample into the microscope, then back to the reactor for sequential reaction experiments. Figure 5 shows the reactor rod [Figure 5(a)] and the rod tip [Figure 5(b–d)]. The tip contains a recess to allow a small disc that would hold a specimen grid to be installed, as shown in Figure 5(c). By manipulating the control knob at the end of the rod, thin sheets of phosphor-bronze spring stock can be slid above and below the specimen grid, allowing the grid to be encapsulated in an inert gas (with a metal-to-metal seal) during the transfer. Experiments utilizing the new capability on the ACEM for reaction studies will be detailed in forthcoming quarterly reports.

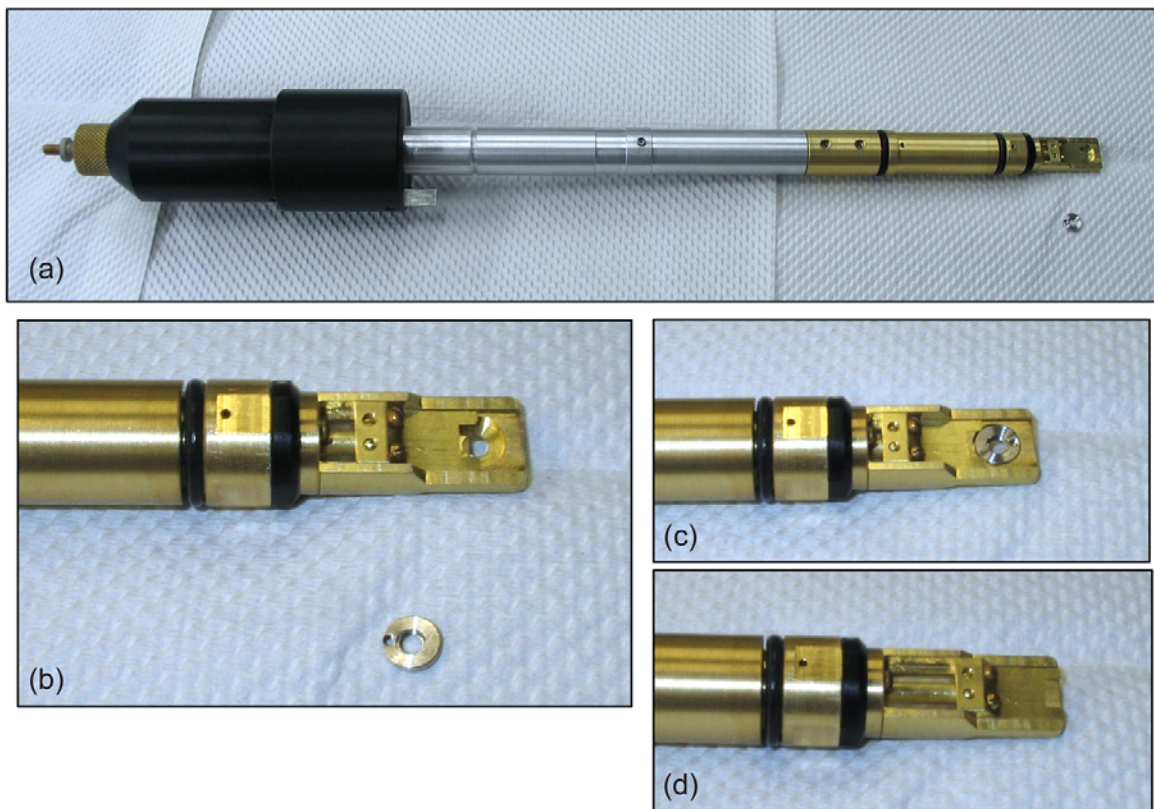


Figure 5. (a) Specimen rod designed for use with the ACEM to permit catalyst reaction studies in the HTML ex-situ reactor system. Tip details shown below. (b) Tip of specimen rod with disc to hold specimen grid adjacent. (c) Rod tip with disc in place. (d) Rod manipulated to position thin metal sheets above and below the specimen (metal-to-metal seal), allowing encapsulation of the sample in an inert gas.

Analysis of Supplier Catalysts

In partnership with colleagues at Ford Research Laboratory and the National Transportation Research Center (NTRC), catalyst materials including lean NO_x trap (LNT) and diesel particulate NO_x reduction (DPNR) materials have been characterized in a program to understand the structures and behavior of catalysts being used in vehicles overseas (Europe). The LNT materials were supplied by Umicore Co. [their GDI (gasoline direct injection) catalyst] and by Toyota (their Avensis D-CAT, or Diesel Clean Advanced Technology catalyst). Toyota also supplied DPNR material for their Avensis vehicle. These materials were characterized initially in the “fresh” or as-received condition, with general microstructure and chemistry provided by electron microprobe analysis, and further high-resolution imaging and microanalysis using the Hitachi TEM and dedicated STEM instruments in

the HTML, as well as the ACEM for ultra-high resolution imaging.

A full presentation of the results of the supplier catalyst studies is beyond the scope of this report, but a few interesting observations are shown as examples. The first observation using the electron microprobe in backscattered electron imaging (BSE) mode showed the Umicore LNT catalyst bulk structure to be a standard single washcoat deposition on a porous cordierite monolith having channels with square cross section. Figure 6(a) shows a typical BSE image of a corner of washcoat, where several blocky aggregate phases are evident (in BSE mode, lighter contrast reflects higher average atomic number of the phase, so baria would be lighter in contrast than alumina, for example). The Toyota D-CAT LNT structure was similar (not shown here), except a cordierite monolith having channels with hexagonal cross section was employed.

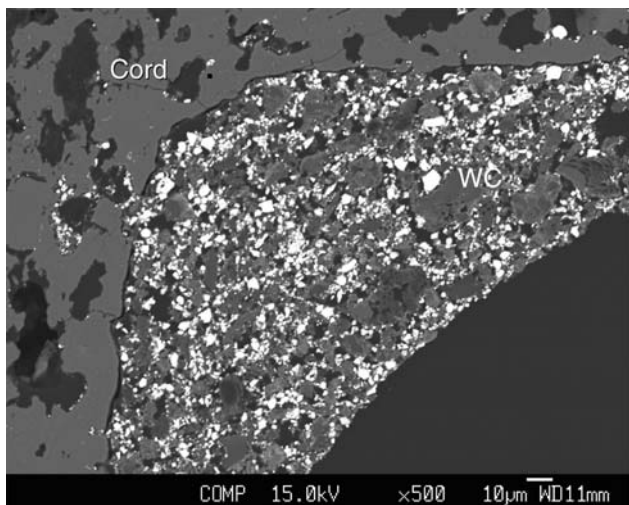


Figure 6. BSE image of corner of a channel in Umicore LNT catalyst monolith, showing single-layer washcoat composed of blocky aggregates of constituents including alumina, baria-alumina and ceria-zirconia.

In contrast to these more standard materials, the Toyota DPNR catalyst utilized a more highly porous monolith structure, and the washcoat material was much finer grained and infiltrated within the pore structure, with none remaining on the channel walls, as illustrated in Figure 6(b) and 6(c). The DPNR structure proved difficult to thin for TEM work, so

results of the study of that material will be reported in a future quarterly. The LNT catalysts were prepared for TEM analysis by standard ion milling techniques, so thin sections of the washcoat were available for high-resolution imaging (see Figure 7).

The Fresh Umicore LNT structure comprised alumina, baria-alumina, and ceria-zirconia (primarily ceria) phases, with platinum as the primary heavy-metal catalytic species. Interestingly, both the alumina and baria-alumina phases contained magnesia (MgO) as a significant constituent (at the 10 wt % level), which is not typical of similar catalysts from other manufacturers. The role of MgO is not yet clear.

The Fresh Umicore material showed a dispersion of platinum clusters and ultra-fine particles that were best imaged with the ACEM, as particles ranged from the 1- to 1.5-nm size range (widely dispersed) down to uniformly dispersed clusters at the near single atom level. After a “de-greening” treatment (standard practice for LNT catalysts), the platinum dispersion was observed in the Hitachi HD-2000 STEM with ADF imaging to form discrete particles in the 2- to 10-nm size range. Images at roughly equivalent magnifications from the ACEM [Figure 8(a)] and the dedicated STEM [Figure 8(b)] illustrate this particle growth. The advantages of

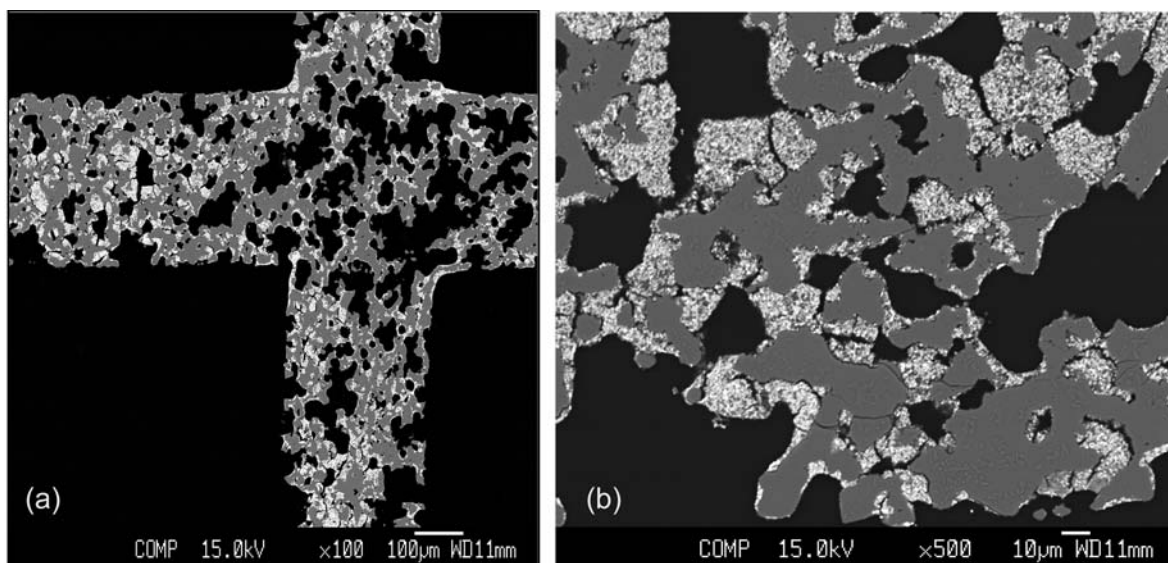


Figure 7. (a) Low-magnification image of polished cross section of Toyota DPNR catalyst structure, showing infusion of washcoat throughout pores of the cordierite monolith. (b) DPNR structure at higher magnification (compare to Figure 6). Washcoat (light contrast) is very fine grained relative to the aggregate structure of the LNT washcoat seen in Figure 6. Black areas are embedding media, and grey areas are cordierite.

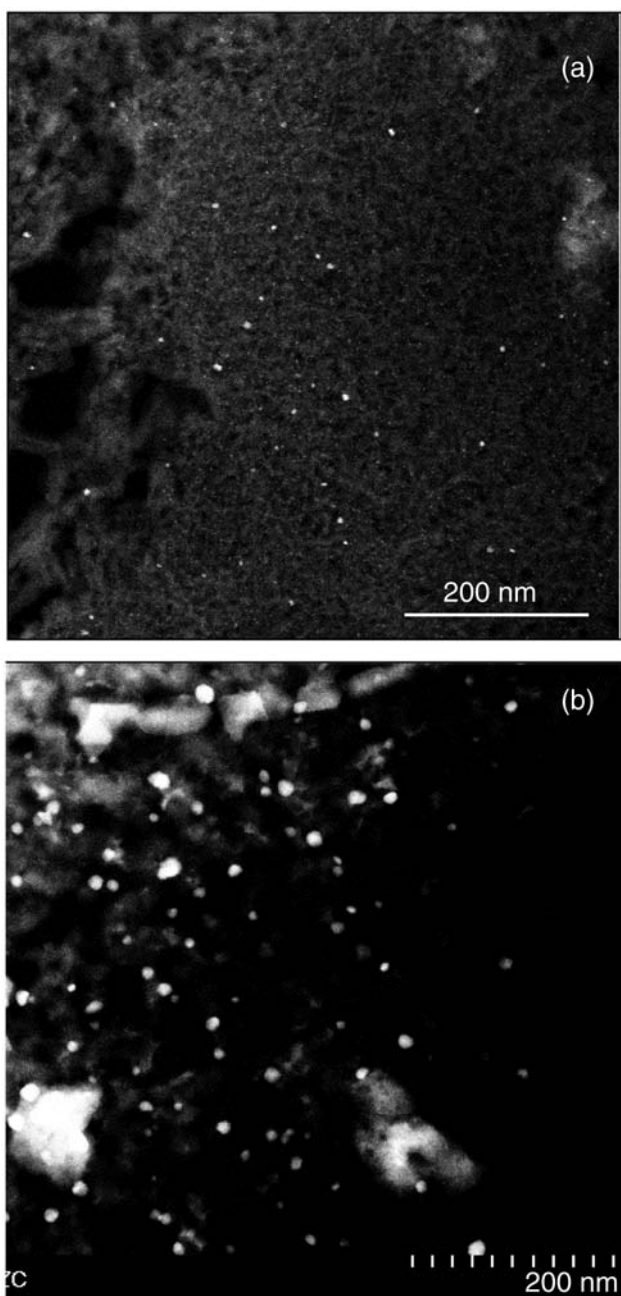


Figure 8. (a) High-resolution ACEM ADF image of ultra-fine platinum clusters level in “Fresh” Umicore LNT catalyst, in area of alumina phase. (b) ADF image from HD-2000 STEM showing particle after a “de-greening” treatment.

imaging heavy-metal particles in the dark-field mode, both with the dedicated STEM for standard resolution imaging and with the new aberration-corrected instrument are clear. The effective change in platinum particle morphologies with further treatments in a benchtop reactor should serve to permit further understanding of the degradation in performance of these LNT catalysts, and will be reported in later quarterlies.

References

1. M. A. O’Keefe, E. C. Nelson, and L. F. Allard, “Focal Series Reconstruction of Nanoparticle Exit Surface Wave,” *Microscopy and Microanalysis*, 2003.

Presentations and Publications

L. F. Allard and C. K. Narula, “Electron Microscopy of LNT Materials: Microstructural Changes with Aging,” Presentation at 2005 CLEERS Workshop, Dearborn, Michigan, May 2005.

V. A. Bhirud, M. J. Moses, D. A. Blom, L. F. Allard, T. Aoki, S. Mishina, C. K. Narula, and B. C. Gates, “Alumina-supported Tri-rhenium Clusters Revealed by Aberration-corrected Electron Microscopy,” *Microscopy and Microanalysis* (2005) (First Place Award winner in Physical Sciences competition).

C. K. Narula, L. F. Allard, M. J. Moses, Y. Xu, W. Shelton, W. F. Schneider, G. Graham, and J. Hoard, “Lean NO_x Traps—Microstructural Studies of Real World and Model Catalysts,” DEER 2005, Palmer Hilton, Chicago, August 21–25, 2005.

M. A. O’Keefe, L. F. Allard, and D. A. Blom, “HRTEM Imaging of Atoms at Sub-Ångström Resolution,” *Journal of Electron Microscopy*, Special Issue in Memory of Prof. John M. Cowley, p. 1–12, August 25, 2005.

M. A. O’Keefe, L. F. Allard, and D. A. Blom, “Resolution Quality and Atom Positions in Sub-Ångström Electron Microscopy,” *Microscopy and Microanalysis*, in press.